NEUROSCIENCE

Carbonic anhydrase 4 disruption decreases synaptic and behavioral adaptations induced by cocaine withdrawal

Subhash C. Gupta[1,2], Ali Ghobbeh[1,2], Rebecca J. Taugher-Hebl[1,2], Rong Fan[1,2], Jason B. Hardie[1,2], Ryan T. LaLumiere[3,4,5], John A. Wemmie[1,2,4,5,6,7,8]*

Cocaine use followed by withdrawal induces synaptic changes in nucleus accumbens (NAc), which are thought to underlie subsequent drug-seeking behaviors and relapse. Previous studies suggest that cocaine-induced synaptic changes depend on acid-sensing ion channels (ASICs). Here, we investigated potential involvement of carbonic anhydrase 4 (CA4), an extracellular pH-buffering enzyme. We examined effects of CA4 in mice on ASIC-mediated synaptic transmission in medium spiny neurons (MSNs) in NAc, as well as on cocaine-induced synaptic changes and behavior. We found that CA4 is expressed in the NAc and present in synaptosomes. Disrupting CA4 either globally, or locally, increased ASIC-mediated synaptic currents in NAc MSNs and protected against cocaine withdrawal–induced changes in synapses and cocaine-seeking behavior. These findings raise the possibility that CA4 might be a previously unidentified therapeutic target for addiction and relapse.

INTRODUCTION

Accumulating evidence suggests substance use disorders are sustained by neuroadaptations in reward circuits produced by repeated drug exposure and withdrawal, which lead to craving and relapse (*1*–*3*). The nucleus accumbens (NAc) is a key hub in the reward circuit where many drug-induced adaptations have been observed (*3*–*5*). For example, in response to cocaine withdrawal, NAc core medium-spiny neurons (MSNs) undergo adaptations such as increases in dendritic spine density, AMPA receptor to *N*-methyl-D-aspartate (NMDA) receptor ratio (AMPAR/NMDAR ratio), and insertion of GluA2-lacking Ca^{2+}-permeable AMPARs (CP-AMPARs) (*6*–*9*). Together, these synaptic rearrangements are thought to contribute to addiction-related behaviors including drug seeking (*10*, *11*).

Our group recently identified a novel regulator of synaptic physiology in the NAc, the acid-sensing ion channel-1A (ASIC1A) (*11*). ASICs are cation channels activated by extracellular acidosis. They form trimeric complexes consisting of ASIC1A, ASIC2A, and ASIC2B, with the ASIC1A subunit being required for activation by pH changes within the physiological range (from pH 7.4 to pH 5) (*12*, *13*). We and others identified a novel component of the EPSC that depended on ASIC1A and extracellular pH buffering, suggesting that ASIC1A is activated by protons released during neurotransmission (*11*, *14*, *15*). Loss of ASIC1A also led to functional and structural rearrangements in NAc core MSNs, including increases in dendritic spine density, AMPAR/NMDAR ratio, frequency of miniature EPSCs (mEPSCs), and rectification index (*11*). These rearrangements resembled adaptations in NAc core MSNs following cocaine withdrawal. In addition, loss of ASIC1A increased sensitivity of AMPAR/NMDAR ratio to a single dose of cocaine, suggesting that ASICs oppose cocaine-evoked plasticity (*11*). Likely related to these synaptic effects, loss of ASIC1A also increased cocaine-reinforced behaviors, including cocaine conditioned place preference (CPP) (*11*). Supporting these observations, others reported a heightened cocaine-evoked locomotor response in cocaine-withdrawn *Asic1a*$^{-/-}$ mice (*16*). Consistent with effects of ASIC1A disruption in mice, overexpressing ASIC1A in rats in the NAc core reduced cocaine self-administration (*11*), raising the exciting possibility that enhancing ASIC1A function might reduce drug-seeking behavior. Subsequent work, however, suggested that overexpressing ASIC1A in rats in NAc core following cocaine self-administration and withdrawal increased reinstatement of cocaine-seeking behavior (*17*). Thus, behavioral effects of potentiating ASIC1A function may be complex.

Another strategy for increasing ASIC activation is to decrease pH buffering capacity. Reducing pH buffering or deleting the critical pH buffering enzyme, carbonic anhydrase 4 (CA4) increases ASIC1A-mediated EPSCs in NAc MSNs (*11*). CA4 is one of 15 CA isoforms that catalyze the reversible pH buffering reaction ($H^+ + HCO_3^- \leftrightarrow CO_2 + H_2O$) (*18*, *19*). Among these isoforms, CA4 is one of the most abundant in brain and is expressed in neurons, glia, and capillary endothelia (*20*, *21*). CA4 is located extracellularly, attached to the cell membrane via a glycosylphosphatidylinositol anchor (*22*), where it has been suggested to contribute to pH buffering at synapses (*21*, *23*, *24*).

On the basis of this prior work, the present study investigated the effects of CA4 disruption on cocaine-induced synaptic physiology, spine morphology, and behavior. We hypothesized that because CA4 disruption increases synaptic ASIC currents, it might produce effects opposite those observed with ASIC1A disruption and thus might protect against the effects of cocaine withdrawal thought to sustain cocaine-seeking behaviors and relapse.

RESULTS

To characterize CA4 in the NAc, we tested protein lysates prepared from NAc tissue punches by Western blot analysis. An anti-CA4 antibody detected a protein of the expected size (~35 kD) in *Car4*$^{+/+}$

[1]Department of Psychiatry, University of Iowa, Iowa City, IA, USA. [2]Department of Veterans Affairs Medical Center, Iowa City, IA, USA. [3]Department of Psychological and Brain Sciences, University of Iowa, Iowa City, IA, USA. [4]Iowa Neuroscience Institute, University of Iowa, Iowa City, IA, USA. [5]Interdisciplinary Graduate Program in Neuroscience, University of Iowa, Iowa City, IA, USA. [6]Department of Molecular Physiology and Biophysics, University of Iowa, Iowa City, IA, USA. [7]Medical Scientist Training Program, University of Iowa, Iowa City, IA, USA. [8]Department of Neurosurgery, University of Iowa, Iowa City, IA, USA.
*Corresponding author. Email: john-wemmie@uiowa.edu

mice, which was absent in *Car4*$^{-/-}$ mice (fig. S1A), indicating the presence of CA4 in NAc and confirming antibody specificity and loss of CA4 protein following gene disruption. To further characterize CA4 distribution in brain tissue, we Western blotted CA4 protein in whole-tissue lysates, membrane-enriched brain fractions, and synaptosome-enriched brain fractions (Fig. 1A). CA4 protein was detected in all three fractions from *Car4*$^{+/+}$ mice but not *Car4*$^{-/-}$ mice. Cofractionation with several synaptic proteins, including PSD-95, GluA1, and ASIC1A, served as positive controls for synaptosome enrichment (*13*, *25*). Myelin basic protein (MBP) and glial fibrillary acidic protein (GFAP) were tested as negative controls (*26*), and as expected, these nonsynaptic proteins were markedly reduced in the synaptosomal fraction (fig. S1B) compared to whole-tissue lysate. These results support the association of CA4 with the cell membrane, as previously reported (*27*). Moreover, they suggest that CA4 is present in synaptosomes and thus might be located near the synapse in relative proximity to other synaptic proteins and receptors.

To determine effects of CA4 on synaptic function, we examined excitatory postsynaptic currents (EPSCs) in NAc MSNs in brain slices. Presynaptic stimulation evoked prominent EPSCs in both *Car4*$^{+/+}$ and *Car4*$^{-/-}$ mice, suggesting that glutamatergic synaptic transmission onto NAc MSNs was largely intact. A component of the EPSC was insensitive to glutamate and γ-aminobutyric acid receptor antagonists. This current constituted about 5% of the total peak EPSC and was significantly greater, about 10% of total peak EPSC, in *Car4*$^{-/-}$ mice (Fig. 1, B and C). Moreover, this current was blocked by the ASIC inhibitor amiloride (Fig. 1B, blue traces) and was absent in double-knockout mice lacking both CA4 and ASIC1A (Fig. 1, B and C). To test whether the effect of CA4 on this synaptic current was through its pH buffering action, we increased the buffering

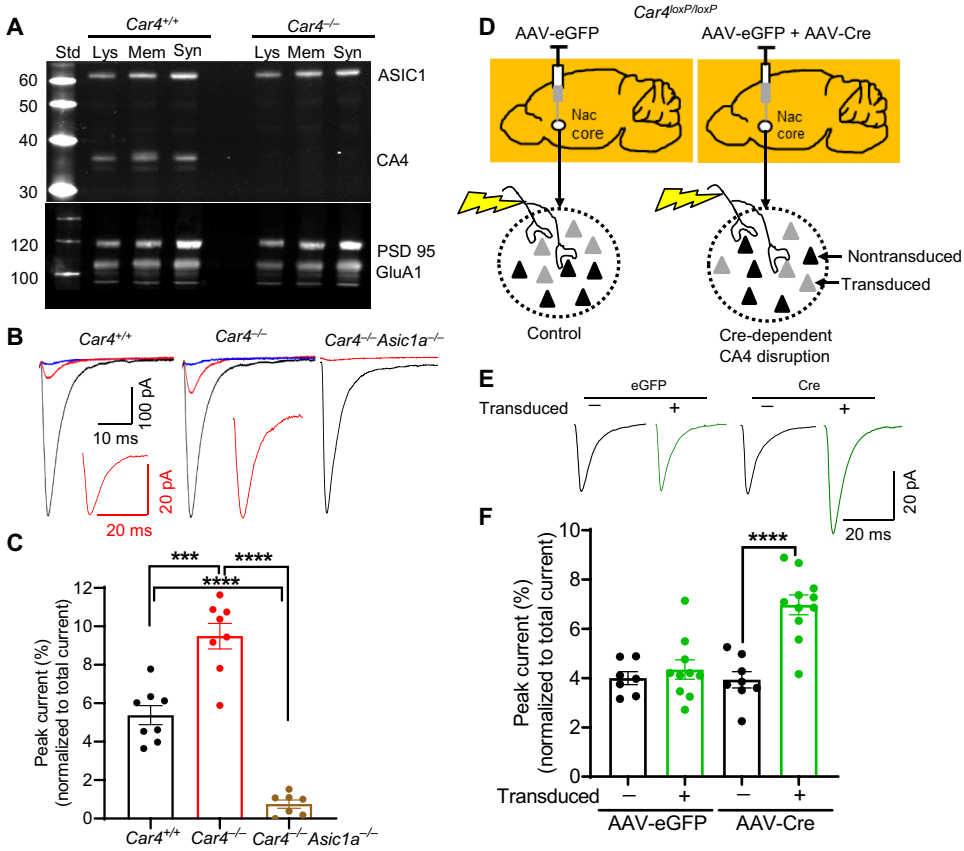

Fig. 1. CA4 is expressed in synaptosomes, and disrupting CA4 in NAc MSNs increased ASIC-dependent synaptic current. (**A**) Western blotting CA4 in whole-brain lysate (Lys), membranes (Mem), and synaptosomal fractions (Syn) from *Car4*$^{+/+}$ and *Car4*$^{-/-}$ mice. CA4 protein (green, top) was absent in samples from *Car4*$^{-/-}$ mice. Similar levels of synaptic proteins ASIC1 (top), PSD 95, and GluR1 (bottom) were expressed in both genotypes and were enriched in membrane and synaptosome fractions relative to whole-brain lysate. (**B**) Representative traces of evoked EPSCs: in the absence of inhibitors (black), in the presence of AP-V, CNQX, and picrotoxin (red), and in the presence of AP-V, CNQX, picrotoxin, and amiloride (blue). Inset: Higher-magnification EPSC component that was sensitive to amiloride but insensitive to AP-V, CNQX, and picrotoxin. (**C**) ASIC-dependent synaptic currents were markedly increased in *Car4*$^{-/-}$ mice relative to *Car4*$^{+/+}$ controls. *Car4*$^{-/-}$ versus *Car4*$^{+/+}$, $t(14) = 4.949$, $^{***}P = 0.0002$, and $n = 8$ neurons from four mice for each genotype. However, in *Car4*$^{-/-}$*Asic1a*$^{-/-}$ mice, this current was significantly reduced compared to *Car4*$^{-/-}$ and *Car4*$^{+/+}$ mice. *Car4*$^{+/+}$ versus in *Car4*$^{-/-}$*Asic1a*$^{-/-}$, $t(13) = 8.10$ and $^{****}P < 0.0001$; *Car4*$^{-/-}$ versus *Car4*$^{-/-}$*Asic1a*$^{-/-}$, $t(13) = 11.8$, $^{****}P < 0.0001$, and $n = 7$ neurons from three mice in *Car4*$^{-/-}$*Asic1a*$^{-/-}$ mice. (**D**) Diagram illustrating experimental strategy. AAV-eGFP or AAV-eGFP + AAV-Cre were injected into the NAc core of *Car4*$^{loxP/loxP}$ mice. Both transduced (gray) and nontransduced (black) neurons were studied. (**E**) Representative traces of ASIC-dependent EPSCs (in the presence of AP-V, CNQX, and picrotoxin) from neurons transduced with indicated vectors (green) or nontransduced (black). (**F**) ASIC-dependent EPSC was increased in Cre-transduced neurons [interaction, $F(1, 32) = 12.44$ and $P = 0.0013$; planned contrasts: AAV-eGFP transduced versus nontransduced, $P = 0.54$ and $n = 7$ and 10 neurons from six mice; AAV-Cre transduced versus nontransduced, $^{***}P < 0.0001$ and $n = 8$ and 11 neurons from six mice].

capacity of the extracellular solution, without changing pH, by increasing the concentrations of HCO_3^- and CO_2 in the artificial cerebrospinal fluid (ACSF). Supporting the likelihood that CA4 disruption affected ASIC1A-dependent EPSCs by reducing pH buffering at synapses, increasing buffering capacity nearly eliminated the current (fig. S2, A and B). Together, these observations suggest that CA4 affects synaptic transmission in the NAc, particularly the ASIC-dependent EPSC, most likely through its pH buffering action.

Conceivably, CA4 located in either the presynaptic, postsynaptic, or extrasynaptic membrane could influence pH buffering at synapses. Of these possibilities, the postsynaptic membrane would be closest to postsynaptic receptors and perhaps best positioned regulate ASICs. To determine whether the postsynaptic neuron might be a key site of CA4 action, we took advantage of newly developed *Car4*$^{loxP/loxP}$ mice. We delivered Cre recombinase plus enhanced green fluorescent protein (eGFP) to MSNs in the NAc core, as described previously (*11*). As a negative control, we delivered an adeno-associated virus (AAV) expressing eGFP alone in a separate group of mice. We hypothesized that if postsynaptic neurons were a key site of CA4 action, then neurons transduced with both Cre and eGFP would exhibit increased ASIC-dependent EPSCs following glutamate receptor blockade compared to neurons transduced with eGFP alone or nontransduced neurons (Fig. 1, D to F). This is what we found (Fig. 1F). These results suggest that targeted disruption of CA4 specifically in postsynaptic neurons was sufficient to produce EPSC effects resembling whole-animal gene disruption. Furthermore, these results suggest that any remaining CA4 that may have been expressed in presynaptic neurons, or other nearby cells, was insufficient to compensate for CA4 loss in postsynaptic neurons.

To further investigate the possible impact of CA4 on synapses in the NAc core, we tested several other measures of synaptic transmission. The AMPAR/NMDAR ratio has received increasing attention as a marker of cocaine-induced plasticity as it likely plays a critical role in drug-seeking behaviors (*28*, *29*). Furthermore, in previous studies, we found that loss of ASIC1A and the associated ASIC1A-dependent EPSC were accompanied by an increased AMPAR/NMDAR ratio in drug-naïve mice (*11*). Therefore, we anticipated that the increased ASIC-dependent EPSC observed following CA4 disruption might have the opposite effect and reduce AMPAR/NMDAR ratio in drug naïve mice. In contrast to this expectation, we found no effect of CA4 disruption on AMPAR/NMDAR ratio in the drug-naïve state (saline withdrawal) (Fig. 2, A to C). To determine the effect of CA4 disruption with regard to cocaine-induced changes in this ratio, we used a protocol previously shown to increase the AMPAR/NMDAR ratio in wild-type mice (*11*, *28*, *30*); we administered cocaine [10 mg/kg, intraperitoneally (i.p.)] for 7 days, followed by 7 days of withdrawal. As expected, repeated cocaine injections followed by withdrawal significantly increased AMPAR/NMDAR ratio in *Car4*$^{+/+}$ mice in both sexes. Notably, cocaine withdrawal failed to increase the AMPAR/NMDAR ratio in *Car4*$^{-/-}$ mice in both sexes (Fig. 2C and fig. S3, A and B). To determine whether this effect was due to CA4 in the NAc, we disrupted CA4 in postsynaptic MSNs in the NAc core in adult *Car4*$^{loxP/loxP}$ mice by transducing them with AAV-Cre and AAV-eGFP (Fig. 2, D to G). Cocaine withdrawal increased the AMPAR/NMDAR ratio in nontransduced neurons and in neurons transduced with eGFP alone but not in neurons transduced with Cre (Fig. 2, F and G). Together, these results suggest that CA4 disruption in NAc core MSNs is sufficient to prevent cocaine withdrawal–induced changes in AMPAR/NMDAR ratio. Further, this effect of CA4 disruption is not due to abnormal brain development because it was elicited after development in adult mice.

One mechanism known to increase AMPAR/NMDAR ratio is a change in AMPAR subunit composition. Cocaine withdrawal increases GluA2-lacking, Ca^{2+}-permeable AMPARs (CP-AMPARs) in the postsynaptic membrane. These receptors are readily identifiable by their increased rectification index and sensitivity to blockade by 1-naphthyl acetyl spermine (NASPM) (*8*, *9*, *31*–*34*). Here, we observed no differences in rectification index or NASPM sensitivity in drug-naïve (saline withdrawn) *Car4*$^{-/-}$ mice compared to their *Car4*$^{+/+}$ counterparts (Fig. 3, A to E, and fig. S3, C to F), suggesting that CA4 disruption by itself does not alter AMPAR subunit composition. However, cocaine withdrawal significantly increased both the rectification index and NASPM sensitivity in *Car4*$^{+/+}$ mice but not in *Car4*$^{-/-}$ mice (Fig. 3, B to E, and fig. S3, C to F). Thus, as with AMPAR/NMDAR ratio, CA4 disruption prevented cocaine-elicited increases in CP-AMPARs in postsynaptic MSNs.

To assess whether CA4 disruption affected AMPAR-mediated EPSC amplitude, we assessed mEPSCs, thereby bypassing presynaptic stimulation and minimizing possible effects of presynaptic excitability. We found that in the drug-naïve state, mEPSC amplitude did not differ between *Car4*$^{+/+}$ and *Car4*$^{-/-}$ mice (Fig. 4, A and B). Cocaine withdrawal significantly increased mEPSC amplitude in *Car4*$^{+/+}$ mice in both sexes (fig. S4, A and B) and consistent with increased CP-AMPARs, reduced mEPSC decay time (Fig. 4C). *Car4*$^{-/-}$ mice were resistant to both withdrawal-induced changes (Fig. 4, A and C, and fig. S4, A and B). Notably, a withdrawal-associated increase in mEPSC frequency was also observed in *Car4*$^{+/+}$ mice that was not seen in *Car4*$^{-/-}$ mice in both sexes (Fig. 4D and fig. S4, C and D). Differences in mEPSC frequency may reflect differences in synapse number or differences in presynaptic release.

To examine possible effects of CA4 and cocaine withdrawal on synapse number, we analyzed dendritic spine density and morphology in drug-naïve versus cocaine-withdrawn *Car4*$^{+/+}$ and *Car4*$^{-/-}$ mice. Previous studies suggested that cocaine withdrawal increases dendritic spine density in the NAc core, largely by increasing immature thin and stubby spines (*6*, *35*–*39*). Consistent with those reports, we found that cocaine withdrawal significantly increased density of total in both sexes (Fig. 5, A and B, and fig. S5A), thin (Fig. 5, C and D), and stubby spines (Fig. 5E) in *Car4*$^{+/+}$ mice, whereas mature mushroom spine density was unchanged (Fig. 5F). In *Car4*$^{-/-}$ mice, we did not expect to find any differences in dendritic spines at baseline because most of our electrophysiological measures of synaptic function at baseline were normal. However, we observed several differences in saline-withdrawn *Car4*$^{-/-}$ mice relative to their *Car4*$^{+/+}$ counterparts: Total, thin, and stubby spine densities were reduced, while mushroom spine density was increased. These differences suggest that CA4 disruption can affect spine structure independent of cocaine exposure. Because *Car4*$^{-/-}$ mice had been resistant to effects of cocaine withdrawal measured thus far, we hypothesized that *Car4*$^{-/-}$ mice would also be resistant to withdrawal-induced changes in dendritic spines. Contrary to this hypothesis, cocaine withdrawal increased density of total (Fig. 5B and fig. S5B), thin (Fig. 5D), and stubby spines (Fig. 5E) in *Car4*$^{-/-}$ mice, although the densities did not reach levels observed in *Car4*$^{+/+}$ mice. The effect of cocaine-withdrawal was independent of sex (fig. S4B). Cocaine withdrawal reduced mushroom spine density in *Car4*$^{-/-}$ mice toward the baseline levels in *Car4*$^{+/+}$ mice. These withdrawal-associated changes in *Car4*$^{-/-}$ mice suggest

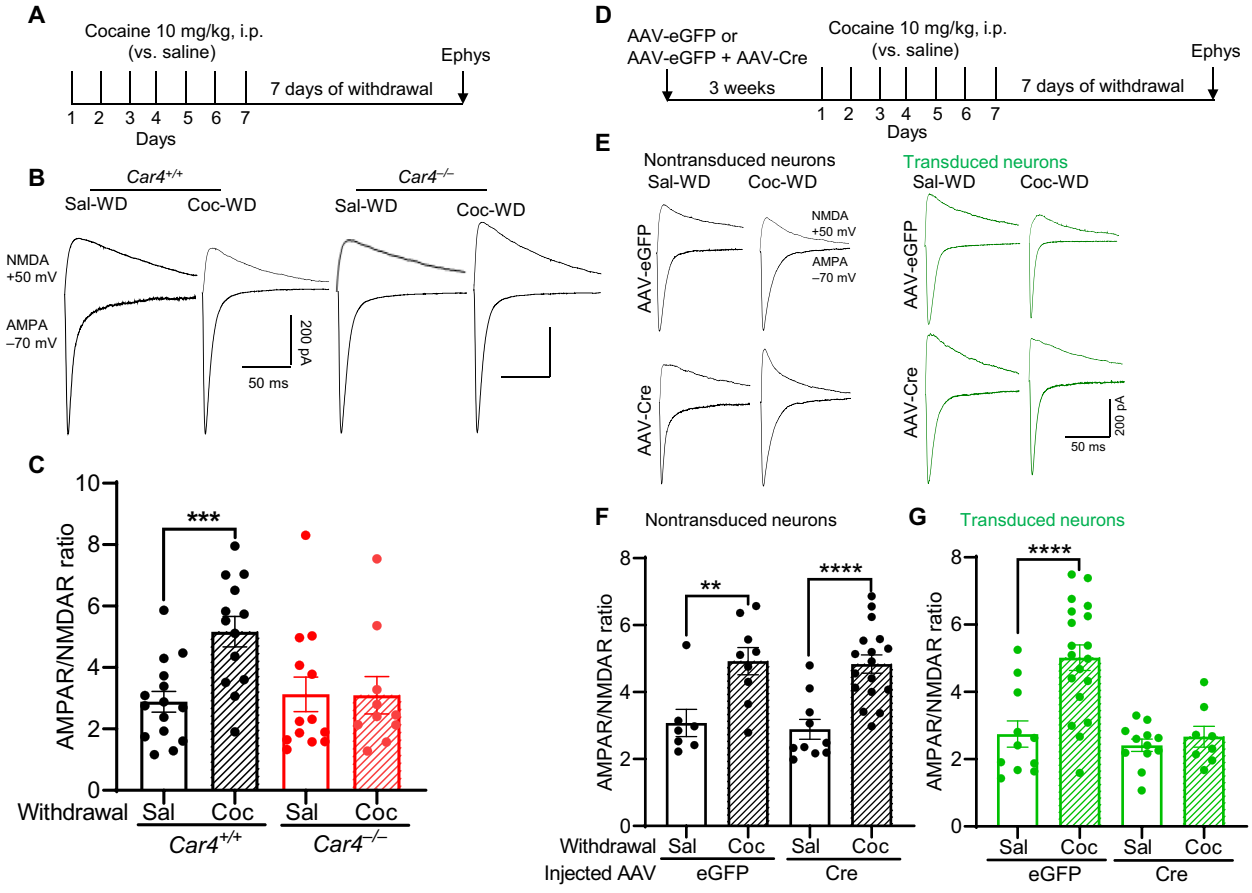

Fig. 2. Disrupting CA4 in NAc MSNs prevented cocaine withdrawal-induced changes in AMPAR/NMDAR. (**A**) Experimental timeline: Cocaine (10 mg/kg, i.p.) or saline (i.p.) was administered in the home cage each day for 7 days followed by 7 days of withdrawal, after which slice electrophysiology was performed. (**B**) Representative traces of the AMPAR-mediated EPSC at −70 mV and the NMDAR-mediated EPSC at +50 mV from *Car4*$^{+/+}$ and *Car4*$^{-/-}$ mice following withdrawal from cocaine (Coc-WD) versus saline (Sal-WD). (**C**) Cocaine withdrawal (Coc) increased AMPAR/NMDAR ratio in *Car4*$^{+/+}$ but not in *Car4*$^{-/-}$ [interaction, $F(1, 48) = 5.9$ and $P = 0.018$; planned contrasts: Coc versus Sal *Car4*$^{+/+}$, $^{**}P = 0.0007$ and $n = 13$ neurons from five mice and 15 neurons from five mice, respectively; Coc versus Sal *Car4*$^{-/-}$, $P = 0.97$ and $n = 10$ neurons from five mice and 13 neurons from five mice, respectively]. (**D**) Experimental timeline. (**E**) Representative traces of AMPAR (−70 mV)– and NMDAR (+50 mV)–evoked EPSCs from transduced and nontransduced neurons in NAc core MSNs of AAV-eGFP– or AAV-Cre + AAV-eGFP–injected *Car4*$^{loxP/loxP}$ mice from Coc-WD or Sal-WD. (**F**) Cocaine withdrawal significantly increased AMPAR/NMDAR ratio in nontransduced neurons [interaction, $F(1, 39) = 0.021$ and $P = 0.883$; planned contrasts: Coc versus Sal non–eGFP-transduced, $^{**}P = 0.0013$ and $n = 9$ neurons from four mice and 7 neurons from four mice, respectively; Coc versus Sal non–Cre-transduced, $^{****}P < 0.0001$ and $n = 17$ neurons from six mice and 10 neurons from five mice, respectively]. (**G**) Cocaine withdrawal did not increase AMPAR/NMDAR ratio in *Car4*$^{loxP/loxP}$ neurons transduced with AAV-Cre [interaction, $F(1, 46) = 7.024$ and $P = 0.011$; planned contrasts: Coc versus Sal Cre-transduced, $P = 0.66$ and $n = 8$ neuron from five mice and 12 neurons from five mice, respectively; Coc versus Sal eGFP-transduced, $^{****}P < 0.0001$ and $n = 19$ neurons from six mice and 11 neurons from five mice, respectively].

that CA4 disruption does not prevent all effects of cocaine withdrawal. In *Car4*$^{+/+}$ mice, the concomitant increase in both spine density and mEPSC frequency supports the likelihood that the number of functioning synapses is increased following withdrawal (*28*, *40*). However, in *Car4*$^{-/-}$ mice, the withdrawal-associated spine changes without significant changes in mEPSC amplitude or frequency suggest that the spine changes are less likely to produce functional effects.

Our results thus far indicated that CA4 disruption influenced synapse structure and function, especially following cocaine withdrawal. These observations raised the question of whether CA4 disruption affects synaptic plasticity in general. To address this question independent of cocaine withdrawal, we stimulated NAc slices from drug-naïve (saline withdrawn) *Car4*$^{+/+}$ and *Car4*$^{-/-}$ mice at 10 Hz for 5 min. This stimulation protocol has been previously shown to induce long-term depression (LTD) at NAc synapses (*41*, *42*). We found that this protocol induced similar levels of LTD in both *Car4*$^{+/+}$ and *Car4*$^{-/-}$ mice (Fig. 6, A and B), suggesting that CA4 disruption by itself does not affect this form of synaptic plasticity. Following cocaine withdrawal, others previously reported enhanced LTD by 13-Hz optogenetic stimulation of medial prefrontal cortex (mPFC) projections to NAc, whereas 1-Hz stimulation produced less LTD (*43*). The authors suggested that CP-AMPAR insertion was more potently reversed by mGluR1-dependent LTD induction (10- to 13-Hz stimulation) rather than by NMDAR-dependent LTD induction (1-Hz stimulation) (*43*). Thus, we were interested whether CA4 disruption would affect LTD induction with our 10-Hz protocol following cocaine withdrawal. In wild-type mice, we found a significant increase in LTD following withdrawal (Fig. 6, C and D). However, in *Car4*$^{-/-}$ mice, the LTD following withdrawal did not differ from drug-naïve mice (Fig. 6, B to D). These data suggest that, although

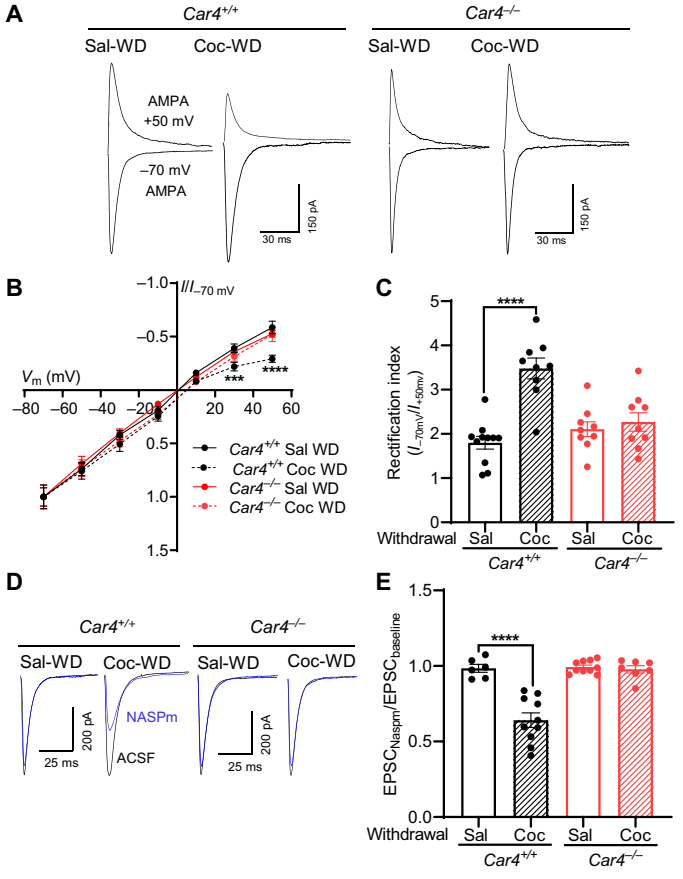

Fig. 3. Disrupting CA4 prevented cocaine withdrawal-induced increases in Ca^{2+}-permeable AMPAR-mediated EPSCs. (**A**) Representative traces of AMPAR-mediated EPSCs at −70 mV and +50 mV in NAc core MSNs of *Car4*$^{+/+}$ and *Car4*$^{-/-}$ mice following cocaine withdrawal (Coc-WD) versus saline withdrawal (Sal-WD). (**B**) Coc-WD produced inward rectification in *Car4*$^{+/+}$ mice but not in *Car4*$^{-/-}$ mice [interaction, $F(6, 87) = 2.213$ $P = 0.049$; planned contrasts: Coc-WD versus Sal-WD *Car4*$^{+/+}$, ****$P < 0.0001$ (at 50 mV), ***$P = 0.0007$ (at 30 mV), and $n = 9$ neurons from four mice and 11 neurons from five mice, respectively; Coc-WD versus Sal-WD *Car4*$^{-/-}$, $P = 0.8961$ (at 50 mV), $P = 0.44$ (at 30 mV), and $n = 7$ neurons from four mice and 6 neurons from four mice, respectively]. (**C**) Rectification index quantification [interaction, $F(1, 34) = 16.10$ and $P = 0.003$; planned contrasts: Coc versus Sal *Car4*$^{+/+}$, ****$P < 0.0001$ and $n = 11$ neurons from five mice and 9 neurons from four mice, respectively; Coc versus Sal *Car4*$^{-/-}$, $P = 0.55$ and $n = 9$ neurons from four mice and 10 neurons from five mice, respectively]. (**D**) Representative traces of the AMPAR-mediated evoked EPSC at −70 mV before (black) and after (blue) NASPM treatment. (**E**) Cocaine withdrawal increased NASPM sensitivity in *Car4*$^{+/+}$ but not in *Car4*$^{-/-}$ mice [interaction, $F(1, 29) = 22.90$ and $P < 0.0001$; planned contrasts: Coc versus Sal *Car4*$^{+/+}$, ****$P < 0.0001$ and $n = 11$ neurons from five mice and 7 neurons from three mice, respectively; Coc versus Sal *Car4*$^{-/-}$, $P = 0.75$ and $n = 7$ neurons from three mice and 10 neurons from five mice respectively].

CA4 disruption may not affect plasticity at baseline, it protected against effects of cocaine withdrawal, consistent with the effects of CA4 disruption on AMPAR/NMDAR ratio, rectification index, NASPM sensitivity, and mEPSCs.

The protective effects of CA4 disruption on the diverse consequences of cocaine withdrawal raised the question of whether cocaine withdrawal might influence CA4 action. To explore this possibility, we tested whether cocaine withdrawal altered CA4 expression in the NAc. We administered cocaine (10 mg/kg, i.p.) versus saline for 7 days followed by 7 days of withdrawal and Western-blotted CA4 protein in NAc tissue punches. CA4 protein levels normalized to a control protein (β-actin) were significantly increased following cocaine withdrawal relative to saline injected control mice (Fig. 7, A and B). This increase in CA4 expression following cocaine withdrawal strengthens the link between CA4 and cocaine and suggests that CA4 action may be especially salient following withdrawal.

Because CA4 disruption influenced synaptic transmission, synaptic plasticity, and spine density in the NAc, we next investigated whether CA4 disruption influenced NAc-dependent or cocaine-reinforced behaviors. We tested locomotor activity in an open-field chamber and found that *Car4*$^{+/+}$ and *Car4*$^{-/-}$ mice exhibited similar levels of activity following saline injection and that an acute cocaine challenge similarly increased locomotor activity in both genotypes (fig. S6, A and B). Targeted disruption of CA4 in the NAc core also had no effect on locomotor activity following acute challenge with saline or cocaine (fig. S6, C and D). These results suggest that baseline locomotor behaviors and baseline locomotor responses to cocaine are not affected by CA4 disruption.

Because the majority of synaptic effects in *Car4*$^{-/-}$ mice were observed after repeated cocaine administration and withdrawal, we then determined whether cocaine withdrawal would lead to behavioral differences. We administered cocaine (10 mg/kg, i.p.) to *Car4*$^{+/+}$ and *Car4*$^{-/-}$ mice for 7 days in the home cage followed by 7 days of abstinence, after which we assessed locomotor responses in the open field to a challenge dose of saline or cocaine (Fig. 8, A and B). Relative to saline, cocaine challenge increased locomotor activity in both genotypes. However, the relative increase was significantly attenuated in *Car4*$^{-/-}$ mice (Fig. 8B and fig. S6E). We performed a similar assessment of locomotor responses following cocaine withdrawal in *Car4*$^{loxP/loxP}$ mice with NAc-targeted CA4 disruption (Fig. 8, C and D, and fig. S6, F to H). Relative to saline, cocaine again induced greater locomotor responses in both CA4 disrupted (AAV-Cre plus AAV-eGFP) and control (AAV-eGFP alone) mice. Also, as with the whole-animal knockouts, disrupting CA4 in NAc significantly reduced the cocaine-associated increase (Fig. 8D). These results suggest that CA4 disruption attenuates the behavioral effects of cocaine following withdrawal and that the NAc is a key site of CA4 action.

We next tested cocaine CPP using a CPP protocol that previously revealed an increase in cocaine CPP in mice lacking ASIC1A (*11*). CA4 disruption had no effect on CPP, as *Car4*$^{+/+}$ and *Car4*$^{-/-}$ mice exhibited similar preferences for the cocaine-paired chamber (fig. S7, A and B). In a separate set of experiments, we also tested cocaine CPP following withdrawal. To parallel the withdrawal protocols above, we performed 7 days of cocaine/saline chamber pairings, followed by 7 days of withdrawal. We then compared changes in place preference at two time points relative to the pretest baseline (fig. S7, C and D). Posttest 1 followed training, while posttest 2 followed an additional 7 days of withdrawal. We found that cocaine CPP did not change significantly between posttest 1 and posttest 2, and there were no significant differences between *Car4*$^{+/+}$ or *Car4*$^{-/-}$ mice (fig. S7D). A similar absence of effect was observed in mice with NAc-targeted CA4 disruption (fig. S7, E and F). However, when we followed the place preference protocol with locomotor testing, we again observed a reduced cocaine-induced locomotor response in mice with CA4 disrupted in NAc (Fig. 8, E and F, and fig. S7G). Together, these results suggest that whereas CA4 disruption reduces locomotor responses to cocaine following withdrawal, CA4 disruption does not affect CPP either pre- or postwithdrawal.

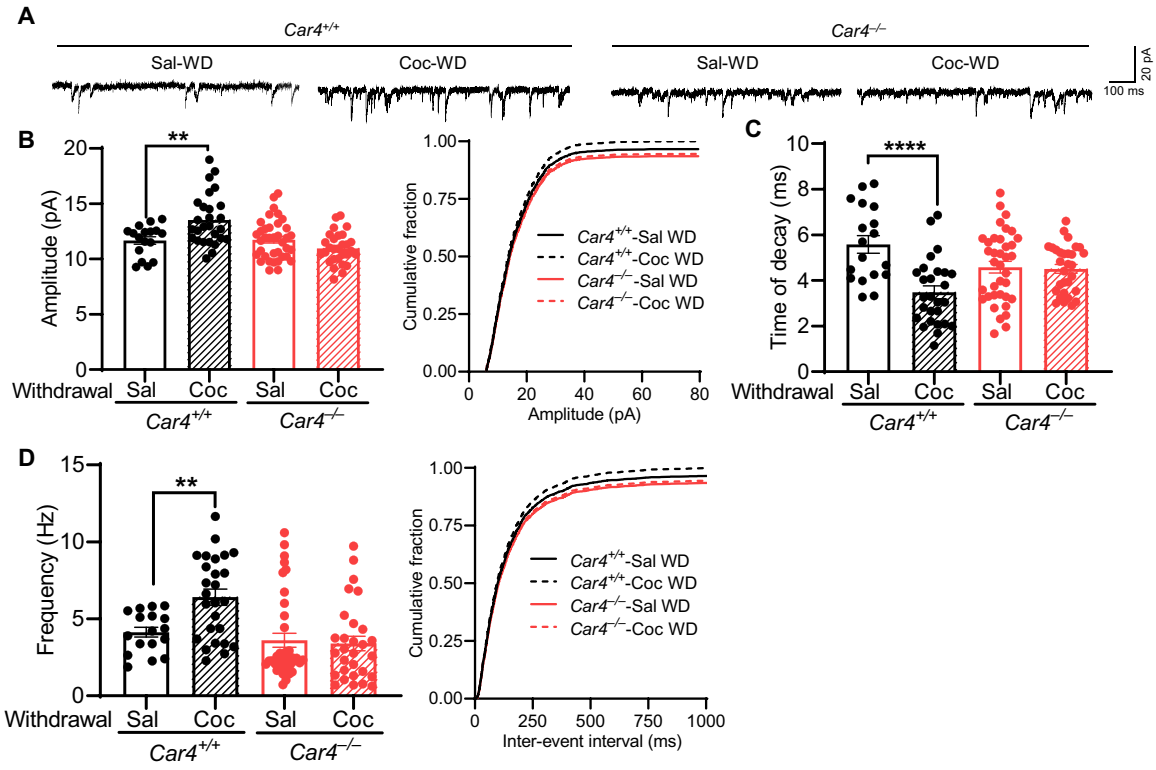

Fig. 4. Disrupting CA4 prevented cocaine withdrawal–induced increases in mEPSC amplitude, decay time, and frequency in NAc MSNs. (**A**) Representative traces of mEPSCs from *Car4*$^{+/+}$ and *Car4*$^{-/-}$ mice after cocaine withdrawal (Coc-WD) and saline withdrawal (Sal-WD). (**B**) Cocaine withdrawal (Coc) increased mEPSC amplitude in *Car4*$^{+/+}$ but not in *Car4*$^{-/-}$ mice [interaction, $F(1, 106) = 13.73$ and $P = 0.0003$; planned contrasts: Coc versus Sal *Car4*$^{+/+}$, $^{**}P = 0.0011$ and $n = 27$ neurons from seven mice and 17 neurons from five mice, respectively; Coc versus Sal *Car4*$^{-/-}$, $P = 0.084$ and $n = 29$ neurons from seven mice and 37 neurons from eight mice, respectively]. (**C**) Cocaine withdrawal reduced mEPSC decay time in *Car4*$^{+/+}$ but not in *Car4*$^{-/-}$ mice [interaction, $F(1, 108) = 13.15$ and $P = 0.0004$; planned contrasts: Coc versus Sal *Car4*$^{+/+}$, $^{****}P < 0.0001$; Coc versus Sal *Car4*$^{-/-}$, $P = 0.83$, sample sizes as in (B)]. (**D**) Cocaine withdrawal increased mEPSC frequency in *Car4*$^{+/+}$ mice but not in *Car4*$^{-/-}$ mice [interaction, $F(1, 105) = 6.237$ and $P = 0.0004$; planned contrasts: Coc versus Sal *Car4*$^{+/+}$, $^{**}P = 0.0042$; Coc versus Sal *Car4*$^{-/-}$, $P = 0.83$, sample sizes as in (B)].

Given that not all cocaine-evoked behaviors were affected by CA4 disruption, we turned to intravenous cocaine self-administration, which is widely acknowledged for modeling addiction, and in which both cocaine self-administration and cocaine-seeking behaviors can be tested (Fig. 9A). We found that *Car4*$^{+/+}$ and *Car4*$^{-/-}$ mice both acquired the ability to self-administer cocaine (Fig. 9, B and C), and both genotypes showed clear preference for the active lever (Fig. 9C). Also, when the infusion dose was reduced, both genotypes exhibited a dose-dependent increase in active lever presses and infusions (Fig. 9, B and C), suggesting that both were motivated to obtain cocaine and to a similar degree. No statistically significant differences between genotypes were observed in amount of drug self-administered or in a baseline test of unreinforced active lever pressing (Fig. 9D and fig. S8). Following 4 weeks of withdrawal, we anticipated that we might see an increase in unreinforced active lever pressing, which would suggest incubation of craving (*1*, *3*, *31*), although this phenomenon has been less reliably observed in mice compared to rats (*44*, *45*). We did not see incubation of craving after withdrawal (Fig. 9D and fig. S8). Instead, the *Car4*$^{+/+}$ mice maintained a similar amount of unreinforced active lever presses that did not differ from baseline (Fig. 9D and fig. S8). In contrast, loss of CA4 significantly reduced unreinforced lever presses after withdrawal, suggesting a decrease in motivation to obtain cocaine. We also tested AMPAR/NMDAR ratio following withdrawal from self-administered cocaine and found that AMPAR/NMDAR ratio was reduced in *Car4*$^{-/-}$ compared to *Car4*$^{+/+}$ mice (Fig. 9, E and F). These results suggest that withdrawal from self-administered cocaine produced synaptic changes resembling withdrawal from experimenter-administered cocaine and that the protective effects of CA4 disruption observed with noncontingent administration also occurred with self-administration and extended beyond 7 days of withdrawal.

DISCUSSION

Together, these studies point to a potentially critical mechanism in the drug-induced synaptic plasticity believed to underlie drug-seeking behavior and relapse. Although CA4 is one of the predominant CA isoforms in brain, few studies have explored its effects on brain function and behavior. Earlier work suggested that CA4 contributes to pH buffering at synapses (*11*, *23*, *46*, *47*). The present findings extend those observations and identify previously unknown roles for CA4 in regulating synaptic transmission and plasticity in NAc and cocaine-seeking behavior.

Protons are concentrated in presynaptic vesicles and are released into the synaptic cleft during neurotransmission, where they influence a variety of pH-sensitive proteins (*14*, *15*, *48*–*50*). The current work detected CA4 in synaptosomes, where its pH buffering action might help counter effects of acid on pH-sensitive receptors. Consistent

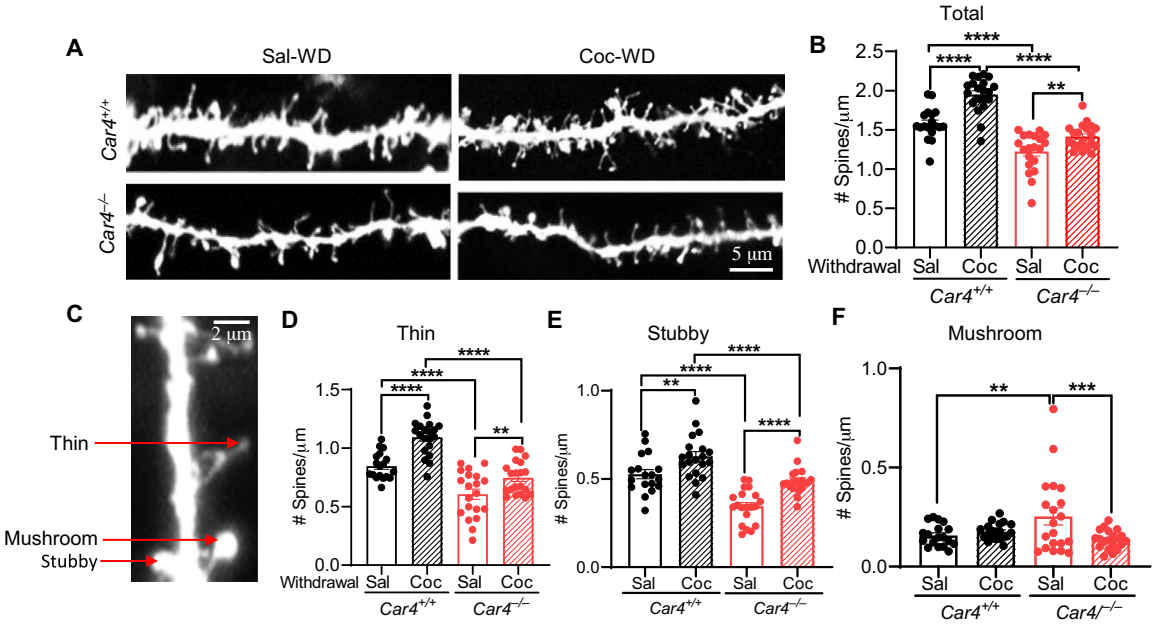

Fig. 5. Cocaine withdrawal and CA4 disruption–induced changes in dendritic spines. (**A**) Representative images of dendritic spines. (**B**) Cocaine withdrawal increased total spine density in $Car4^{+/+}$ mice and also in $Car4^{-/-}$ mice but not to same levels [interaction, $F(1, 74) = 3.66$ and $P = 0.059$; treatment, $F(1, 74) = 35.21$ and $P < 0.0001$; genotype, $F(1, 74) = 88.71$ and $P < 0.0001$, $n = 18$ to 20; planned contrasts: Coc versus Sal $Car4^{+/+}$, ****$P < 0.0001$ and $n = 20$ neurons from five mice and 18 neurons from five mice, respectively; Coc versus Sal $Car4^{-/-}$, **$P = 0.0052$ and $n = 20$ neurons from five mice and 20 neurons from five mice, respectively; $Car4^{+/+}$ versus $Car4^{-/-}$ Sal, ****$P < 0.0001$; $Car4^{+/+}$ versus $Car4^{-/-}$ Coc, ****$P < 0.0001$]. Sample sizes are the same from (D) to (F). (**C**) Examples of stubby, thin, and mushroom spines. (**D**) Thin spines [interaction, $F(1, 74) = 2.377$ and $P = 0.127$; treatment, $F(1, 74) = 31.31$ and $P < 0.0001$; genotype, $F(1, 74) = 72.16$ and $P < 0.0001$; planned contrasts: Coc versus Sal $Car4^{+/+}$, ****$P < 0.0001$; Coc versus Sal $Car4^{-/-}$, **$P = 0.0048$; $Car4^{+/+}$ versus $Car4^{-/-}$ Sal, ****$P < 0.0001$; $Car4^{+/+}$ versus $Car4^{-/-}$ Coc, ****$P < 0.0001$]. (**E**) Stubby spines. [interaction, $F(1, 74) = 0.85$ and $P = 0.35$; treatment, $F(1, 74) = 27.97$ and $P < 0.0001$; genotype, $F(1, 74) = 47.53$ and $P < 0.0001$; planned contrasts: Coc versus Sal $Car4^{+/+}$, **$P = 0.0032$; Coc versus Sal $Car4^{-/-}$, ****$P < 0.0001$; $Car4^{+/+}$ versus $Car4^{-/-}$ Sal, ****$P < 0.0001$; $Car4^{+/+}$ versus $Car4^{-/-}$ Coc, ****$P < 0.0001$]. (**F**) Mushroom spines [interaction, $F(1, 74) = 7.95$ and $P = 0.006$; treatment, $F(1, 74) = 4.189$ and $P = 0.04$; genotype, $F(1, 74) = 1.358$ and $P = 0.24$; planned contrasts: Coc versus Sal $Car4^{+/+}$, $P = 0.59$; Coc versus Sal $Car4^{-/-}$, ***$P = 0.0008$; $Car4^{+/+}$ versus $Car4^{-/-}$ Sal, **$P = 0.006$; $Car4^{+/+}$ versus $Car4^{-/-}$ Coc, $P = 0.23$].

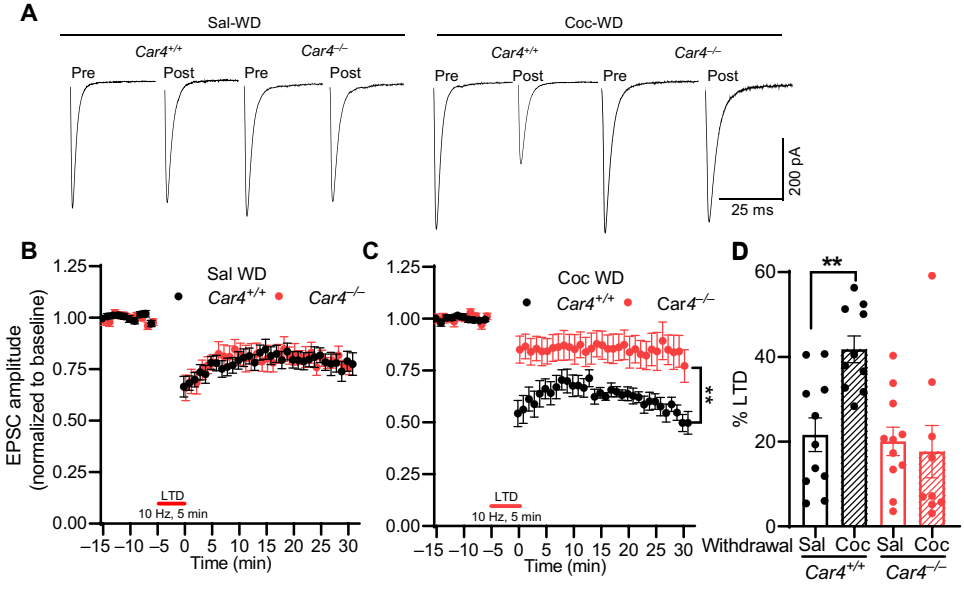

Fig. 6. Disrupting CA4 prevented cocaine withdrawal–induced increase in LTD. (**A**) Representative traces of evoked AMPA EPSCs before and after LTD induction from NAc core MSNs from $Car4^{+/+}$ and $Car4^{-/-}$ mice after cocaine withdrawal (Coc-WD) or after saline withdrawal (Sal-WD). (**B**) After Sal-WD, $Car4^{+/+}$ and $Car4^{-/-}$ mice exhibited a similar degree of LTD (20 to 30 min after induction) [$t(20) = 0.3$, $P = 0.76$, and $n = 11$ neurons from six mice in each genotype]. (**C**) After Coc-WD, $Car4^{+/+}$ mice had greater LTD compared to $Car4^{-/-}$ mice [$t(17) = 3.59$, **$P = 0.0022$, and $n = 10$ neurons from five mice and 9 neurons from five mice, respectively]. (**D**) % LTD quantification [interaction, $F(1, 37) = 7.266$ and $P = 0.0105$; planned contrasts: Coc versus Sal $Car4^{+/+}$, **$P = 0.008$; Coc versus Sal $Car4^{-/-}$, $P = 0.69$].

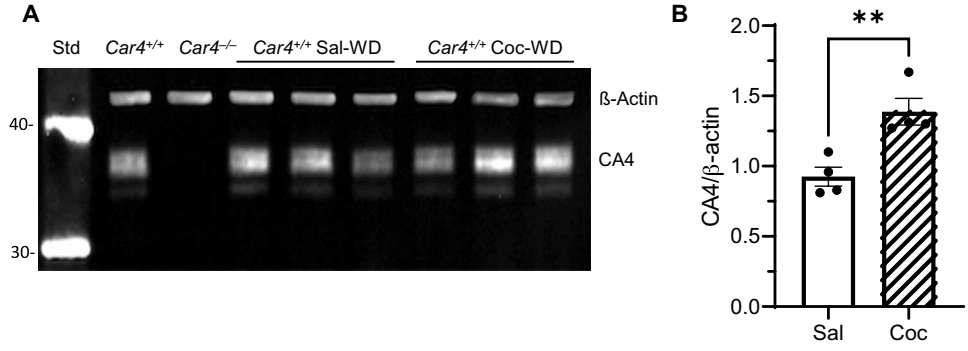

Fig. 7. Cocaine withdrawal increases CA4 expression in the NAc. (**A**) Representative Western blot of CA4 and β-actin in protein lysates of NAc tissue punches from mice of indicated genotypes and treatment groups. (**B**) Cocaine withdrawal increased CA4 protein in NAc relative to saline-treated controls [$t(12) = 3.575$, $^{**}P = 0.0038$, and $n = 7$ per group], and CA4 was absent in $Car4^{-/-}$ NAc.

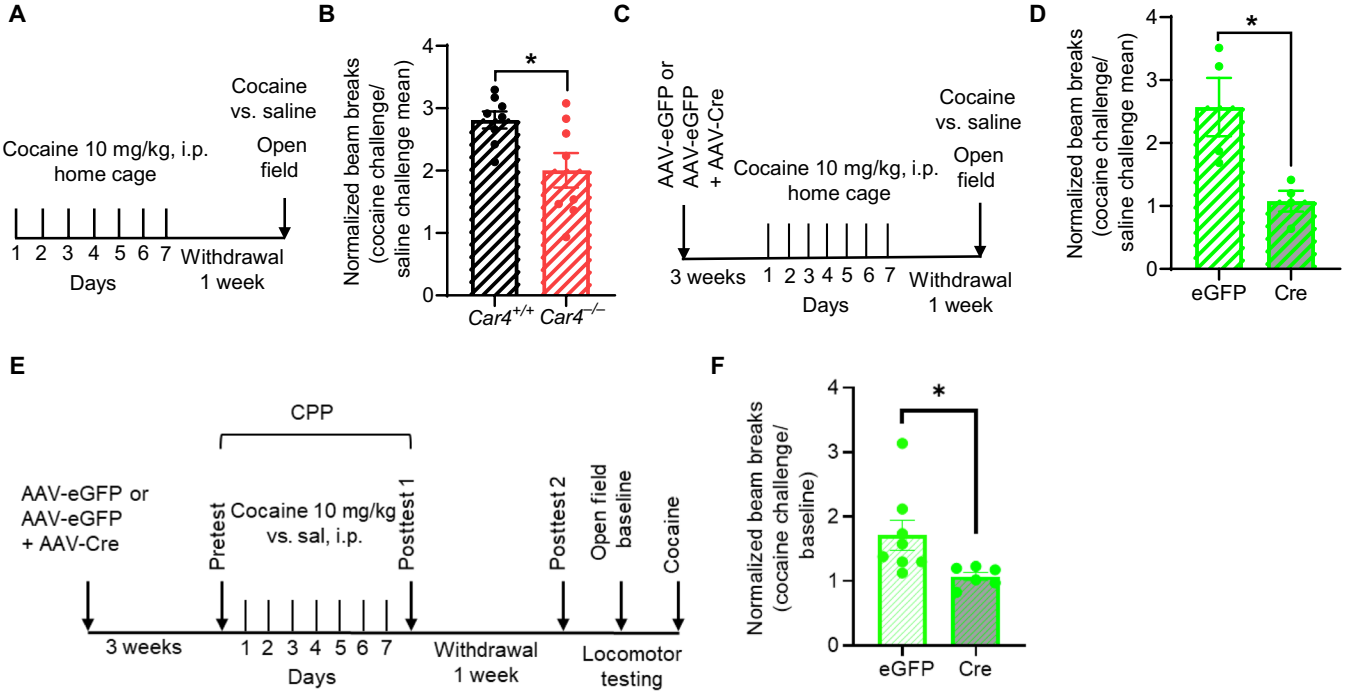

Fig. 8. Whole-animal and NAc-restricted CA4 disruption reduced locomotor responses to acute cocaine challenge after withdrawal. (**A**) Experimental timeline for postwithdrawal locomotor responses to cocaine challenge in $Car4^{+/+}$ and $Car4^{-/-}$ mice. (**B**) After withdrawal, locomotor responses to acute cocaine challenge normalized to acute saline challenge [$Car4^{+/+}$ versus $Car4^{-/-}$, $t(14) = 2.60$, $^{*}P = 0.02$, and $n = 8$ mice per group]. (**C**) Experimental timeline for postwithdrawal locomotor responses to acute cocaine challenge in $Car4^{loxP/loxP}$ mice. (**D**) After cocaine withdrawal, locomotor responses to acute cocaine challenge normalized to acute saline challenge were reduced in $Car4^{loxP/loxP}$ mice transduced in NAc core with AAV-Cre versus AAV-eGFP [$t(6) = 3.038$, $^{*}P = 0.022$, and $n = 4$ mice per group]. (**E**) Experimental timeline of post-withdrawal locomotor responses to cocaine challenge in $Car4^{loxP/loxP}$ mice with AAV-Cre versus AAV-eGFP transduction in NAc core following cocaine CPP. (**F**) Postwithdrawal locomotor responses of the same mice to acute cocaine challenge [AAV-Cre versus AAV-eGFP, $t(12) = 2.316$ and $^{*}P = 0.039$], following cocaine CPP.

with this role, CA4 disruption significantly increased ASIC1A-dependent EPSCs, suggesting that CA4 normally helps to reduce postsynaptic ASIC activation. Moreover, our finding that cocaine withdrawal increased CA4 expression in the NAc suggests CA4 action may be especially important following withdrawal.

Unexpectedly, in drug-naïve mice, CA4 disruption did not affect a number of synaptic measures. These measures included evoked EPSCs, AMPAR/NMDAR ratio, AMPAR rectification, and NASPM sensitivity, as well as amplitude, kinetics, and frequency of AMPA-mediated mEPSCs. Consistent with those findings, LTD, locomotor behavior, and acute locomotor responses to cocaine were also normal in $Car4^{-/-}$ mice at baseline. Only after cocaine withdrawal were the effects of CA4 disruption observed. In contrast, in $Car4^{+/+}$ mice, all of these measures were altered by cocaine withdrawal. Notably, cocaine-withdrawn $Car4^{-/-}$ mice did not differ from drug-naïve $Car4^{-/-}$ mice, suggesting that CA4 disruption prevented a host of

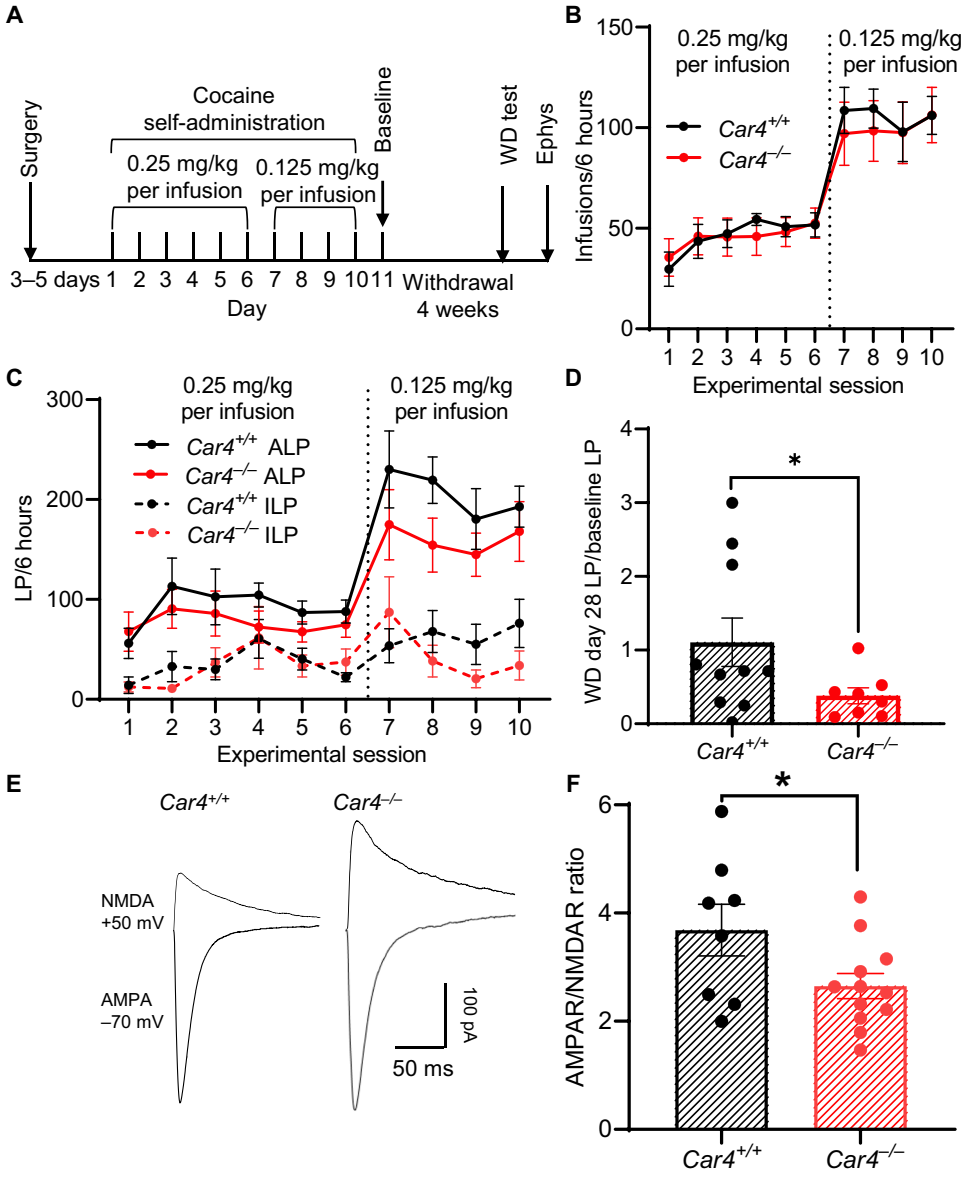

Fig. 9. Following withdrawal from cocaine self-administration, CA4 disruption reduced cocaine seeking, and AMPAR/NMDAR. (**A**) Experimental timeline for intravenous cocaine self-administration. (**B**) Infusions across experimental sessions. There was an effect of cocaine dose on number of infusions [$F(1, 16) = 129.7$, $P < 0.0001$, and $n = 10$, 8 mice per group] but no effect of genotype [$F(1, 16) = 0.0605$ and $P = 0.808$] and no dose × genotype interaction [$F(1, 16) = 0.263$ and $P = 0.614$]. (**C**) Lever presses [active (ALP) and inactive (ILP)] across experimental sessions. There was an effect of cocaine dose on ALP [$F(1, 16) = 94.58$ and $P < 0.0001$] and ILP [$F(1, 16) = 5.87$ and $P = 0.027$] but no effect of genotype ($Car4^{+/+}$ versus $Car4^{-/-}$) on ALP [$F(1, 16) = 1.257$ and $P = 0.27$] or ILP [$F(1, 16) = 0.352$ and $P = 0.5610$] and no dose × genotype interaction on ALP [$F(1, 16) = 2.151$ and $P = 0.161$] or ILP [$F(1, 16) = 0.9314$, $P = 0.348$]. (**D**) Cocaine seeking (unreinforced ALP) in postwithdrawal test normalized to pre-withdrawal baseline. CA4 disruption reduced postwithdrawal cocaine seeking [$Car^{+/+}$ versus $Car4^{-/-}$, one-tailed, $t(10) = 2.722$ and $^*P = 0.029$]. (**E**) Representative traces of AMPAR (−70 mV) and NMDAR (+50 mV) from NAc core of $Car4^{+/+}$ and $Car4^{-/-}$ mice recorded after withdrawal from cocaine self-administration and behavioral testing. (**F**) AMPAR/NMDAR ratio was reduced in $Car4^{-/-}$ versus $Car4^{+/+}$ mice [one-tailed, $t(18) = 2.15$, $^*P = 0.022$, and $n = 12$ neurons from three mice and 8 neurons from two mice, respectively].

cocaine-induced synaptic abnormalities. These results suggest that pH buffering by CA4 intersects with synaptic plasticity mechanisms associated with cocaine exposure and withdrawal.

It is not yet clear exactly how repeated cocaine exposure followed by withdrawal produces this complex array of synaptic abnormalities. It has been suggested that cocaine withdrawal reduces mGluR1 expression and/or signaling, which reduces downstream IP3-mediated Ca^{2+} release and diacylglycerol-dependent protein kinase C activation resulting in greater CP-AMPAR trafficking to the postsynaptic membrane (*7*, *34*, *51*). Supporting this mechanism, mGluR1 agonists have been found to reverse withdrawal-induced synaptic changes (*34*, *51*), and mGluR1-dependent LTD protocols increased removal of CP-AMPARs at mPFC to D1-MSN synapses (*43*). Among these mGluR1-dependent mechanisms, CA4 disruption seems most likely to compensate for reduced Ca^{2+} release. We showed here that CA4 disruption increases ASIC1A activation at synapses. Moreover,

consistent with previous results (*15*, *52*–*54*), we found that extracellular acid induced large increases in intracellular Ca^{2+} in NAc MSNs, which were absent in *Asic1a*$^{-/-}$ mice and were eliminated by blocking voltage-gated Ca^{2+} channels (VGCCs) with Cd^{2+} (fig. S9, A to C). Together, these results support a model whereby CA4 disruption increases ASIC1A activation, which, in turn, raises intracellular Ca^{2+} via VGCCs, which may oppose the reduced Ca^{2+} signaling previously described following cocaine withdrawal (*34*, *51*).

Although CA4 disruption may influence a variety of pH-dependent signaling mechanisms, ASICs appear to mediate many of the effects. Besides their exquisite pH sensitivity, we previously found that ASIC1A disruption produced many of the same synaptic rearrangements as cocaine withdrawal (*11*). Results herein suggest that enhancing ASIC activation at synapses via CA4 disruption may lead to effects opposite those of ASIC1A loss. This was reflected in the effects of CA4 disruption on dendritic spines. In drug-naïve mice, CA4 disruption reduced total, thin, and stubby spines, whereas previous work observed that ASIC1A disruption increased total, thin, and stubby spines (*11*). However, the increased mushroom spines in CA4 knockouts found in the present study are inconsistent with this pattern, as the prior work found that ASIC1A disruption had no effect on mushroom spine density (*11*). Thus, although a number of effects of CA4 disruption were consistent with what might be predicted from previous findings with ASIC1A disruption, some were not and might thus be mediated by other pH-sensitive targets.

One expectation not borne out by these experiments was the hypothesized effect on cocaine CPP. Because loss of ASIC1A increased CPP, we hypothesized that the ability of CA4 disruption to increase ASIC-mediated synaptic currents would decrease CPP to below normal levels. The absence of effect suggests that CPP may not be bidirectionally sensitive to ASIC manipulation. Or perhaps there are other consequences of CA4 disruption that can counteract increased ASIC activity. Other compensatory mechanisms independent of CA4 may also come into play. Nonetheless, divergence between CPP and other drug-seeking behaviors including intravenous self-administration is not unprecedented (*55*, *56*), and several important behavioral consequences of CA4 disruption were still observed.

In three separate experiments, CA4 disruption reduced cocaine-evoked locomotor responses following withdrawal (Fig. 8, B, D, and F). Also, most relevant to drug-seeking behavior in humans, in cocaine self-administration studies, mice lacking CA4 had a significant reduction in cocaine-seeking behavior after 4 weeks of withdrawal, whereas before withdrawal, *Car4*$^{-/-}$ mice behaved similarly to *Car4*$^{+/+}$ mice. For example, cocaine-evoked locomotor responses at baseline, self-administration tested at two different doses of cocaine, and initial cocaine-seeking 1 day after self-administration were all normal. Thus, both synaptic and behavioral effects of CA4 disruption were specific to the postwithdrawal period, when an ability to prevent relapse could have considerable impact.

In conclusion, the experiments in this manuscript substantially advance the understanding of CA4 in brain and its importance in synaptic physiology and behavior. Critically, these studies suggest that disrupting CA4 prevents insidious synaptic changes likely critical for sustaining the addiction cycle. Although more work is needed to better understand these findings, they raise the intriguing possibility that disrupting or inhibiting CA4 in the brain has important value in treating substance use disorders.

MATERIALS AND METHODS

Mice

Mice used for all the experiments were on a C57BL/6J genetic background and were matched for age and sex. *Car4*$^{+/+}$ and *Car4*$^{-/-}$ mice (stock no. 008217) (*23*) were obtained from The Jackson Laboratory. *Asic1a*$^{-/-}$ mice were generated as previously described (*57*). The *Car4*$^{-/-}$*Asic1a*$^{-/-}$ double-knockout mice were generated by crossing *Car4*$^{-/-}$ and *Asic1a*$^{-/-}$ mice. *Car4*$^{loxP/loxP}$ mice were generated by intercrossing C57BL/6NTac-*Car4*$^{tm1a(EUCOMM)Wtsi}$/Ieg mice (European Mouse Mutant Archive) with B6.129S4-*Gt (ROSA)26Sor*$^{tm1(FLP1)Dym}$/RainJ mice (The Jackson Laboratory, stock no. 009086) (fig. S10A). This intercross excised the LacZ and neomycin resistance cassettes, thereby converting the *Car4*-null tm1a allele to a conditional knockout tm1c allele. Excision of the LacZ and neomycin resistance cassettes was detected via polymerase chain reaction (PCR; fig. S10, B to D). Primers 1 and 2 were used to detect the presence of the cassettes. Primers 1 and 3 were used to detect the excision of the cassettes: primer 1 (GACAATGAATGACACTGGGAG), primer 2 (CAACGGGTTCTTCTGTTAGTCC), primer 3 (ACTTCATGATGCTGAGCTCTG). All mice were housed in groups of two to five littermates, kept on a standard 12-hour light-dark cycle, and fed standard chow and water ad libitum. Experiments were performed during the light cycle, and all groups were matched for sex and age (10 to 15 weeks). Animal care met the National Institutes of Health standards, and the University of Iowa Animal Care and Use Committee approved all experiments. In experiments where automated scoring was not available, experimenters were blinded to genotype and condition.

Western blotting

Protein lysates were prepared by homogenizing whole-brain tissue in cold lysis buffer containing phosphate-buffered saline, 1% Triton X-100, and protease inhibitors (Roche Complete, Mini), centrifugation at 5000 rpm for 10 min, followed by supernatant collection, and Western blotted as previously described (*11*). Synaptosomes and membrane fractions were prepared from whole brain as previously described (*58*). NAc punches (1.2 mm in diameter) around the anterior commissure were collected from coronal sections (thickness, 2 mm). Primary antibodies included rabbit anti-ASIC1 polyclonal antiserum (MTY19) diluted 1:3000 (*59*), rabbit anti-glutamate receptor 1 polyclonal antibody (Millipore, AB1504) diluted 1:1000, goat anti-CA4 polyclonal antibody (R&D Systems, AF2414) diluted 1:1000, mouse anti-PSD95 monoclonal antibody (clone K28/43, catalog no. 05-494, Upstate) diluted 1:300, rabbit anti-MBP monoclonal antibody (Abcam, 218001) diluted 1:1000, and mouse anti-GFAP (Millipore, MAB360) diluted 1:1000. Secondary antibodies (diluted 1:10,000 to 1:20,000) included IRDye 680LT donkey anti-rabbit immunoglobulin G (IgG; LI-COR, 926-68023), IRDye 800CW donkey anti-rabbit IgG (LI-COR, 926-32213), IRDye 800CW donkey anti-goat IgG (LI-COR, 926-32214), and IRDye 680LT donkey anti-mouse IgG (LI-COR, 926-68022). Membranes were imaged with an Odyssey imaging system (LI-COR).

Slice preparation and electrophysiology

As previously described (*11*), briefly, 300-μm coronal NAc brain slices were prepared from 8- to 12-week-old mice in ice-cold slicing buffer (225 mM sucrose, 26 mM $NaHCO_3$, 1.2 mM KH_2PO_4, 1.9 mM KCl, 10 mM D-glucose, 1.1 mM $CaCl_2$, and 2 mM $MgSO_4$) bubbled with 95% O_2 and 5% CO_2. Slices were transferred to oxygenated ACSF

(127 mM NaCl, 26 mM $NaHCO_3$, 1.2 mM KH_2PO_4, 1.9 mM KCl, 10 mM D-glucose, 2.2 mM $CaCl_2$, and 2 mM $MgSO_4$) held at 32°C for 30 min followed by 30 min at room temperature (RT) for recovery. Whole-cell recordings of MSN neurons were performed using 2.5- to 4-megohm pipettes. Recordings were obtained using an Axopatch 200B amplifier (Axon Instruments) and analyzed offline by Clampfit (Axon software). Experiments were discarded if access resistance varied by more than 20%.

Evoked EPSCs

Internal recording solution consisted of the following: 125 mM cesium methanesulfonate, 20 mM CsCl, 10 mM NaCl, 2 mM Mg–adenosine 5′-triphosphate (ATP), 0.3 mM Na–guanosine 5′-triphosphate (GTP), 10 mM Hepes, 0.2 mM EGTA, and 2.5 mM QX314, pH 7.3 adjusted with CsOH. EPSCs were evoked using a bipolar tungsten electrode. ASIC-dependent EPSCs were recorded at −70 mV in the presence of picrotoxin (100 μM), 6-cyano-7-nitroquinoxaline-2,3-dione (CNQX; 20 μM), and AP-V (100 μM). Amiloride (500 μM) was used to inhibit ASIC-EPSCs (all chemicals from Sigma-Aldrich). In a separate experiments, $Car4^{-/-}$ mice were tested for ASIC-dependent EPSCs in normal buffering solution (26 mM $HCO_3^{-/-}$ and 5% CO_2) and in solution with increased buffering capacity (70 mM $HCO_3^{-/-}$ and 15% CO_2) without altering the pH. AMPAR/NMDAR ratio of evoked EPSCs was calculated from AMPAR-EPSC amplitude at −70 mV by the NMDAR-EPSC amplitude at +50 mV, using the late component of the NMDAR EPSC, 60 ms after the onset. Both AMPAR and NMDAR EPSCs were recorded in the presence of picrotoxin (100 μM). CNQX (20 μM) was added to the bath to record NMDAR EPSCs. A current-voltage (*I-V*) relationship was plotted to examine AMPAR subunit composition. Following correction of the holding voltage for liquid junction potential (~8 mV), evoked AMPAR-mediated EPSCs were measured at membrane potentials of −70, −50, 0, −30, −10, +10, +30, and +50 mV in the presence picrotoxin (100 μM) and AP-V (100 μM), with spermine (0.1 mM, Sigma-Aldrich) in the internal solution. Rectification index of AMPAR-mediated EPSCs was calculated as ratio of $I_{-70\ mV}$ divided by $I_{+50\ mV}$. AMPAR NASPM sensitivity was determined by collecting 20 to 25 baseline sweeps in ACSF while holding the cell's voltage at −70 mV and 15 min following application of NASPM (200 μM, Alomone Lab). Spermine (0.1 mM) was added to the internal pipette solution during the rectification and NASPM experiments.

Cocaine withdrawal

To test effects of cocaine withdrawal, $Car4^{+/+}$, $Car4^{-/-}$, and $Car4^{loxP/loxP}$ mice were injected with cocaine (10 mg/kg, i.p.) or saline (0.9%, i.p.) in the home cage once daily for 7 days, followed by 7 days of withdrawal. Cocaine was provided by the National Institute on Drug Abuse.

Virus vectors

AAV were injected and targeting was confirmed as previously described (*11*). Briefly, AAV2/1 vectors expressing Cre recombinase or eGFP under the control of a CMV promoter (University of Iowa Gene Transfer Vector Core) were injected bilaterally into the NAc core (relative to bregma: anteroposterior, +1.2 mm; lateral, ±1.0 mm; and ventral, −3.9 mm from the pial surface). At least 3 weeks was allowed for virus transduction before electrophysiological and behavioral testing. The Cre groups included a 70/30 mixture of AAV-CMV-Cre plus AAV-CMV-eGFP to facilitate verification of virus targeting. Hits were confirmed posthoc by bilateral fluorescence in the NAc core with a Zeiss 710 microscope.

Miniature EPSCs

Internal recording solution was as follows: 125 mM potassium gluconate, 10 mM NaCl, 20 mM KCl, 10 mM Hepes, 0.2 mM EGTA, 2 mM Mg-ATP, 0.3 mM Na-GTP, and 2.5 mM QX314, pH 7.3 adjusted with KOH. mEPSCs were recorded at a holding potential of −70 mV in the presence of tetrodotoxin (1 μM, Sigma-Aldrich) and picrotoxin (100 μM). mEPSC frequency, amplitude, and kinetic properties were assessed using the Mini Analysis software package (version 4.3, Synaptosoft).

DiI labeling

Mice were anesthetized with ketamine and xylazine and transcardially perfused with sodium phosphate buffer (PB; 0.1 M, pH 7.4) followed by 50 ml of 1.5% paraformaldehyde (PFA) in 0.1 M PB. Brains were removed and postfixed (same fixative) for 1 hour at RT. Coronal slices (150 μm) were cut on vibratome and collected in PB. DiI, a lipophilic carbocyanine dye (Molecular Probes, Life Technologies, Grand Island, NY, USA), was used to label MSN dendritic spines. DiI crystals were delivered onto surface of NAc core slices by micromanipulator-controlled glass capillary pipette visualized under a dissecting microscope. DiI was allowed to diffuse along dendrites and axons for 48 hours at 4°C in PB containing thimerosal [0.01% (w/v), Sigma-Aldrich]. Labeled sections were then briefly rinsed in PB and fixed in 4% PFA for 1 hour at RT and mounted onto glass slides with Vectashield (Vector Laboratories).

Dendritic spine imaging and analysis

Dendritic segments were imaged with a confocal microscope (Zeiss 710) using 63× oil immersion objective at 0.29 μm by 0.29 μm pixel scale. Nonoverlapping dendritic segments 50 to 150 μm from the soma and with a minimum length of 30 μm were randomly selected for high-resolution imaging (pixel size of 0.07 μm by 0.07 μm) and scanned at 0.1-μm intervals along the *z* axis. Spine analysis was performed as described previously (*11*). Briefly, Neuron Studio was used to characterize individual spine morphology as thin, stubby, or mushroom based on head/neck diameter and spine length and for spine density quantification. The following experimental groups were composed of five animals per group, four neurons per animal, and two to four dendritic segments per neuron, with assessed total spine number in parentheses: $Car4^{+/+}$ saline (4583), $Car4^{+/+}$ cocaine withdrawal (6291), $Car4^{-/-}$ saline (3947), and $Car4^{-/-}$ cocaine withdrawal (4561).

LTD induction

LTD in NAc was induced using an established protocol NAc (*41*, *42*). Briefly, LTD was induced with 10-Hz stimulation for 5 min at −50 mV, and LTD magnitude was determined by normalizing the average EPSC amplitude 30 min after induction to the baseline EPSC amplitude recorded during the 10 min immediately preceding LTD induction.

Locomotor activity

Locomotor responses to acute challenges of cocaine (10 mg/kg, i.p.) or vehicle (0.9% saline) were assessed on indicated days for 30 min via infrared beam breaks in open-field chambers (San Diego Instruments). To test the effects of withdrawal, mice first received daily

injections of cocaine (10 mg/kg, i.p) or vehicle (0.9% saline) for 7 days in home cage, followed by 7 days with no injections.

Cocaine CPP

CPP to cocaine (10 mg/kg, i.p.) was assessed as previously described (*11*), with figures indicating relevant timelines. To assess the effects of withdrawal, CPP was assessed 1 day after the final cocaine injection and after 1 week of withdrawal, as indicated.

Cocaine self-administration

Under anesthesia with ketamine, xylazine, and isoflurane, catheters (silicone tubing, 0.31 mm inner diameter and 0.64 mm outer diameter, Dow Corning Silastic) connected to stainless steel guide cannulae (22G, Plastics One) were surgically implanted ~1 mm into the jugular vein and anchored with 5-0 silk sutures. Guide cannulae were anchored to the skull with bone screws, epoxy, and dental cement. To reduce infection, prophylactic enrofloxacin (5 mg/kg, i.p.) was administered postoperatively for 7 days. Catheter patency was verified with sodium methohexital infusions (2%, 20 μl). Mice displaying no sedation within 3 s were excluded from further experimentation. One day before initiating self-administration, mice were fasted overnight and subsequently restricted to 85 to 90% of their prefast body weight through sessions 1 to 10. For 6-hour self-administration sessions, mice were connected to intravenous infusion pumps in operant chambers (Med Associates, St. Albans, VT), where active lever presses triggered a 1-s cocaine infusion on a fixed-ratio 1 schedule [0.25 mg/kg (sessions 1 to 6) and 0.125 mg/kg (sessions 7 to 10)], as well activation of tone and white light above the active lever for 20 s, during which additional infusions could not be obtained. Maximum cocaine dose was capped at 15 mg/kg per 6-hour session. Inactive levers produced no response. To motivate lever pressing, food dust was initially placed on the active lever during sessions 1 and 2. For inclusion in the final dataset, mice were required to meet 2 performance criteria during two of the last three training sessions: (i) at least 10 infusions per session and (ii) active lever pressing greater than inactive lever pressing. Both $Car4^{+/+}$ and $Car4^{-/-}$ mice preferred the active lever during this time period [one-sample *t* test, $Car4^{+/+}$ mice: $t(9) = 4.773$ and $P = 0.0010$; $Car4^{-/-}$ mice: $t(7) = 5.425$ and $P = 0.0010$]. Cocaine-seeking behavior was subsequently assessed during two 30-min test sessions: one at baseline (24 hours after the final self-administration session) and the second after 4 weeks of withdrawal, during which active lever presses resulted in cue presentations, but no cocaine infusions.

Calcium imaging and analysis

Ca^{2+}-sensitive indicator Fluo-4 (100 μM) and Ca^{2+}-insensitive indicator Alexa Fluor 568 (50 μM) in a gluconate-based intracellular solution were dialyzed into the cells through a patch recording pipette. Imaging was performed in the presence of 100 μM picrotoxin, 20 μM CNQX, 50 μM d-APV, 2 mM 4-AP, and 20 mM tetraethylammonium chloride. Acidic ACSF (buffered with 10 mM 4-morpholineethanesulfonic acid and titrated to pH 5.6 with NaOH) was applied from a pipette positioned ~10 to 30 μM from the cell body using a Femtojet 5247 (Eppendorf) at 1 to 2 psi for 1 s. Epifluorescence signals were captured at a framerate of 33.33 Hz filtered through dichroic cubes with a high-speed complementary metal-oxide semiconductor camera. Signals were analyzed using ImageJ and MATLAB (MathWorks) by summing the fluorescent intensity with a circular region of interest (ROI) drawn around the soma for each frame (*60*). Baseline-subtracted Fluo-4 (green) ROI fluorescence was divided by AF 568 (red) ROI fluorescence and presented as $\%\Delta G/R$.

Verification of loxP site functionality

Cre-mediated recombination of the $Car4^{loxP/loxP}$ allele was verified in $Car4^{loxP/loxP}$ mice bilaterally injected with AAV2/1-CMV-Cre into the NAc. Wild-type mice and $Car4^{loxP/loxP}$ mice bilaterally injected with AAV2/1-CMV-eGFP into the NAc served as controls. Three weeks after injection, bilateral NAc punches were taken, and DNA was isolated using a QiAamp DNA Mini Kit (Qiagen, Hilden, Germany). Excision of the critical region was detected via PCR. Primers 1 and 2 identified and discriminated between wild-type *Car4* and intact $Car4^{loxP/loxP}$ alleles, and primers 1 and 3 detected the excised $Car4^{loxP/loxP}$ allele: primer 1 (TCAGGTCCAGGGTCTTTCCA), primer 2 (AGGCTAGTGGGTCTCTGATGT), and primer 3 (CCCAAGGGAGTTTGGTCCTC).

Statistical analysis

Student's *t* test was used to assess statistical significance for experiments involving two groups. Two-way analysis of variance (ANOVA) was used to assess statistical significance for experiments involving more than two groups. Within the context of the full ANOVA, planned contrast testing was used to test a priori hypothesized relationships between groups. Where indicated, strong directional hypotheses were tested with one-tailed test. ROUT test with $Q = 1\%$ was used to screen for outliers. Because normality tests are underpowered with samples of this size, distributions were assumed normal. *F* test was used to compare variances between groups, and Welch's correction was applied for unequal variances. *P* values less than 0.05 were considered significant. All bar graphs express values as means ± SEM. All statistical analyses were performed using GraphPad Prism 8.4.3.

SUPPLEMENTARY MATERIALS

Supplementary material for this article is available at https://science.org/doi/10.1126/sciadv.abq5058

View/request a protocol for this paper from *Bio-protocol*.

REFERENCES AND NOTES

1. C. Luscher, The emergence of a circuit model for addiction. *Annu. Rev. Neurosci.* **39**, 257–276 (2016).
2. E. J. Nestler, Molecular basis of long-term plasticity underlying addiction. *Nat. Rev. Neurosci.* **2**, 119–128 (2001).
3. M. E. Wolf, Synaptic mechanisms underlying persistent cocaine craving. *Nat. Rev. Neurosci.* **17**, 351–365 (2016).
4. P. W. Kalivas, The glutamate homeostasis hypothesis of addiction. *Nat. Rev. Neurosci.* **10**, 561–572 (2009).
5. M. E. Wolf, The Bermuda Triangle of cocaine-induced neuroadaptations. *Trends Neurosci.* **33**, 391–398 (2010).
6. D. T. Christian, X. Wang, E. L. Chen, L. K. Sehgal, M. N. Ghassemlou, J. J. Miao, D. Estepanian, C. H. Araghi, G. E. Stutzmann, M. E. Wolf, Dynamic alterations of rat nucleus accumbens dendritic spines over 2 months of abstinence from extended-access cocaine self-administration. *Neuropsychopharmacology* **42**, 748–756 (2017).
7. J. A. Loweth, K. Y. Tseng, M. E. Wolf, Adaptations in AMPA receptor transmission in the nucleus accumbens contributing to incubation of cocaine craving. *Neuropharmacology* **76**, 287–300 (2014).
8. J. E. McCutcheon, X. Wang, K. Y. Tseng, M. E. Wolf, M. Marinelli, Calcium-permeable AMPA receptors are present in nucleus accumbens synapses after prolonged withdrawal from cocaine self-administration but not experimenter-administered cocaine. *J. Neurosci.* **31**, 5737–5743 (2011).
9. A. Purgianto, A. F. Scheyer, J. A. Loweth, K. A. Ford, K. Y. Tseng, M. E. Wolf, Different adaptations in AMPA receptor transmission in the nucleus accumbens after short vs long

access cocaine self-administration regimens. *Neuropsychopharmacology* **38**, 1789–1797 (2013).
10. J. L. Cornish, P. W. Kalivas, Glutamate transmission in the nucleus accumbens mediates relapse in cocaine addiction. *J. Neurosci.* **20**, RC89 (2000).
11. C. J. Kreple, Y. Lu, R. J. Taugher, A. L. Schwager-Gutman, J. du, M. Stump, Y. Wang, A. Ghobbeh, R. Fan, C. V. Cosme, L. P. Sowers, M. J. Welsh, J. J. Radley, R. T. LaLumiere, J. A. Wemmie, Acid-sensing ion channels contribute to synaptic transmission and inhibit cocaine-evoked plasticity. *Nat. Neurosci.* **17**, 1083–1091 (2014).
12. C. C. Askwith, J. A. Wemmie, M. P. Price, T. Rokhlina, M. J. Welsh, Acid-sensing ion channel 2 (ASIC2) modulates ASIC1 H^+-activated currents in hippocampal neurons. *J. Biol. Chem.* **279**, 18296–18305 (2004).
13. J. A. Wemmie, R. J. Taugher, C. J. Kreple, Acid-sensing ion channels in pain and disease. *Nat. Rev. Neurosci.* **14**, 461–471 (2013).
14. J. Du, L. R. Reznikov, M. P. Price, X.-m. Zha, Y. Lu, T. O. Moninger, J. A. Wemmie, M. J. Welsh, Protons are a neurotransmitter that regulates synaptic plasticity in the lateral amygdala. *Proc. Natl. Acad. Sci. U.S.A.* **111**, 8961–8966 (2014).
15. C. González-Inchauspe, F. J. Urbano, M. N. Di Guilmi, O. D. Uchitel, Acid-sensing ion channels activated by evoked released protons modulate synaptic transmission at the mouse calyx of held synapse. *J. Neurosci.* **37**, 2589–2599 (2017).
16. Q. Jiang, C. M. Wang, E. E. Fibuch, J. Q. Wang, X. P. Chu, Differential regulation of locomotor activity to acute and chronic cocaine administration by acid-sensing ion channel 1a and 2 in adult mice. *Neuroscience* **246**, 170–178 (2013).
17. A. L. Gutman, C. V. Cosme, M. F. Noterman, W. R. Worth, J. A. Wemmie, R. T. La Lumiere, Overexpression of ASIC1A in the nucleus accumbens of rats potentiates cocaine-seeking behavior. *Addict. Biol.* **25**, e12690 (2020).
18. P. Blandina, G. Provensi, M. B. Passsani, C. Capasso, C. T. Supuran, Carbonic anhydrase modulation of emotional memory. Implications for the treatment of cognitive disorders. *J. Enzyme Inhib. Med. Chem.* **35**, 1206–1214 (2020).
19. C. T. Supuran, Carbonic anhydrase inhibitors and activators for novel therapeutic applications. *Future Med. Chem.* **3**, 1165–1180 (2011).
20. M. S. Ghandour, O. K. Langley, X. L. Zhu, A. Waheed, W. S. Sly, Carbonic anhydrase IV on brain capillary endothelial cells: A marker associated with the blood-brain barrier. *Proc. Natl. Acad. Sci. U.S.A.* **89**, 6823–6827 (1992).
21. N. Svichar, S. Esquenazi, A. Waheed, W. S. Sly, M. Chesler, Functional demonstration of surface carbonic anhydrase IV activity on rat astrocytes. *Glia* **53**, 241–247 (2006).
22. A. Waheed, X. L. Zhu, W. S. Sly, Membrane-associated carbonic anhydrase from rat lung. Purification, characterization, tissue distribution, and comparison with carbonic anhydrase IVs of other mammals. *J. Biol. Chem.* **267**, 3308–3311 (1992).
23. G. N. Shah, B. Ulmasov, A. Waheed, T. Becker, S. Makani, N. Svichar, M. Chesler, W. S. Sly, Carbonic anhydrase IV and XIV knockout mice: Roles of the respective carbonic anhydrases in buffering the extracellular space in brain. *Proc. Natl. Acad. Sci. U.S.A.* **102**, 16771–16776 (2005).
24. N. Svichar, A. Waheed, W. S. Sly, J. C. Hennings, C. A. Hubner, M. Chesler, Carbonic anhydrases CA4 and CA14 both enhance AE3-mediated Cl--HCO3- exchange in hippocampal neurons. *J. Neurosci.* **29**, 3252–3258 (2009).
25. R. A. Nicoll, S. Tomita, D. S. Bredt, Auxiliary subunits assist AMPA-type glutamate receptors. *Science* **311**, 1253–1256 (2006).
26. P. Gulyassy, G. Puska, B. A. Györffy, K. Todorov-Völgyi, G. Juhász, L. Drahos, K. A. Kékesi, Proteomic comparison of different synaptosome preparation procedures. *Amino Acids* **52**, 1529–1543 (2020).
27. A. Waheed, X. L. Zhu, W. S. Sly, P. Wetzel, G. Gros, Rat skeletal muscle membrane associated carbonic anhydrase is 39-kDa, glycosylated, GPI-anchored CA IV. *Arch. Biochem. Biophys.* **294**, 550–556 (1992).
28. S. Kourrich, P. E. Rothwell, J. R. Klug, M. J. Thomas, Cocaine experience controls bidirectional synaptic plasticity in the nucleus accumbens. *J. Neurosci.* **27**, 7921–7928 (2007).
29. M. A. Ungless, J. L. Whistler, R. C. Malenka, A. Bonci, Single cocaine exposure in vivo induces long-term potentiation in dopamine neurons. *Nature* **411**, 583–587 (2001).
30. S. L. Borgland, R. C. Malenka, A. Bonci, Acute and chronic cocaine-induced potentiation of synaptic strength in the ventral tegmental area: Electrophysiological and behavioral correlates in individual rats. *J. Neurosci.* **24**, 7482–7490 (2004).
31. K. L. Conrad, K. Y. Tseng, J. L. Uejima, J. M. Reimers, L. J. Heng, Y. Shaham, M. Marinelli, M. E. Wolf, Formation of accumbens GluR2-lacking AMPA receptors mediates incubation of cocaine craving. *Nature* **454**, 118–121 (2008).
32. C. R. Ferrario, J. A. Loweth, M. Milovanovic, K. A. Ford, G. L. Galiñanes, L. J. Heng, K. Y. Tseng, M. E. Wolf, Alterations in AMPA receptor subunits and TARPs in the rat nucleus accumbens related to the formation of Ca^{2+}-permeable AMPA receptors during the incubation of cocaine craving. *Neuropharmacology* **61**, 1141–1151 (2011).
33. M. Mameli, B. Halbout, C. Creton, D. Engblom, J. R. Parkitna, R. Spanagel, C. Lüscher, Cocaine-evoked synaptic plasticity: Persistence in the VTA triggers adaptations in the NAc. *Nat. Neurosci.* **12**, 1036–1041 (2009).
34. J. E. McCutcheon, J. A. Loweth, K. A. Ford, M. Marinelli, M. E. Wolf, K. Y. Tseng, Group I mGluR activation reverses cocaine-induced accumulation of calcium-permeable AMPA receptors in nucleus accumbens synapses via a protein kinase C-dependent mechanism. *J. Neurosci.* **31**, 14536–14541 (2011).
35. J. I. Giza, Y. Jung, R. A. Jeffrey, N. M. Neugebauer, M. R. Picciotto, T. Biederer, The synaptic adhesion molecule SynCAM 1 contributes to cocaine effects on synapse structure and psychostimulant behavior. *Neuropsychopharmacology* **38**, 628–638 (2013).
36. J. Kim, B. H. Park, J. H. Lee, S. K. Park, J. H. Kim, Cell type-specific alterations in the nucleus accumbens by repeated exposures to cocaine. *Biol. Psychiatry* **69**, 1026–1034 (2011).
37. K. W. Lee, Y. Kim, A. M. Kim, K. Helmin, A. C. Nairn, P. Greengard, Cocaine-induced dendritic spine formation in D1 and D2 dopamine receptor-containing medium spiny neurons in nucleus accumbens. *Proc. Natl. Acad. Sci. U.S.A.* **103**, 3399–3404 (2006).
38. T. E. Robinson, B. Kolb, Structural plasticity associated with exposure to drugs of abuse. *Neuropharmacology* **47**(Suppl 1), 33–46 (2004).
39. X. Wang, M. E. Cahill, C. T. Werner, D. J. Christoffel, S. A. Golden, Z. Xie, J. A. Loweth, M. Marinelli, S. J. Russo, P. Penzes, M. E. Wolf, Kalirin-7 mediates cocaine-induced AMPA receptor and spine plasticity, enabling incentive sensitization. *J. Neurosci.* **33**, 11012–11022 (2013).
40. W. J. Wright, Y. Dong, Silent synapses in cocaine-associated memory and beyond. *J. Neurosci.* **41**, 9275–9285 (2021).
41. B. A. Grueter, G. Brasnjo, R. C. Malenka, Postsynaptic TRPV1 triggers cell type-specific long-term depression in the nucleus accumbens. *Nat. Neurosci.* **13**, 1519–1525 (2010).
42. B. D. Turner, J. M. Rook, C. W. Lindsley, P. J. Conn, B. A. Grueter, mGlu1 and mGlu5 modulate distinct excitatory inputs to the nucleus accumbens shell. *Neuropsychopharmacology* **43**, 2075–2082 (2018).
43. V. Pascoli, J. Terrier, J. Espallergues, E. Valjent, E. C. O'Connor, C. Lüscher, Contrasting forms of cocaine-evoked plasticity control components of relapse. *Nature* **509**, 459–464 (2014).
44. A. L. Nugent, E. M. Anderson, E. B. Larson, D. W. Self, Incubation of cue-induced reinstatement of cocaine, but not sucrose, seeking in C57BL/6J mice. *Pharmacol. Biochem. Behav.* **159**, 12–17 (2017).
45. R. Spanagel, Animal models of addiction. *Dialogues Clin. Neurosci.* **19**, 247–258 (2017).
46. N. Fedirko, M. Avshalumov, M. E. Rice, M. Chesler, Regulation of postsynaptic $Ca2^+$ influx in hippocampal CA1 pyramidal neurons via extracellular carbonic anhydrase. *J. Neurosci.* **27**, 1167–1175 (2007).
47. J. A. Gottfried, M. Chesler, Endogenous H^+ modulation of NMDA receptor-mediated EPSCs revealed by carbonic anhydrase inhibition in rat hippocampus. *J. Physiol.* **478**(Pt 3), 373–378 (1994).
48. G. Miesenböck, D. A. De Angelis, J. E. Rothman, Visualizing secretion and synaptic transmission with pH-sensitive green fluorescent proteins. *Nature* **394**, 192–195 (1998).
49. S. Trapp, M. Lückermann, P. A. Brooks, K. Ballanyi, Acidosis of rat dorsal vagal neurons in situ during spontaneous and evoked activity. *J. Physiol.* **496**(Pt 3), 695–710 (1996).
50. S. Trapp, M. Lückermann, K. Kaila, K. Ballanyi, Acidosis of hippocampal neurones mediated by a plasmalemmal $Ca2^+/H^+$ pump. *Neuroreport* **7**, 2000–2004 (1996).
51. J. A. Loweth, A. F. Scheyer, M. Milovanovic, A. L. LaCrosse, E. Flores-Barrera, C. T. Werner, X. Li, K. A. Ford, T. le, M. F. Olive, K. K. Szumlinski, K. Y. Tseng, M. E. Wolf, Synaptic depression via mGluR1 positive allosteric modulation suppresses cue-induced cocaine craving. *Nat. Neurosci.* **17**, 73–80 (2014).
52. Z. G. Xiong, X. M. Zhu, X. P. Chu, M. Minami, J. Hey, W. L. Wei, J. F. MacDonald, J. A. Wemmie, M. P. Price, M. J. Welsh, R. P. Simon, Neuroprotection in ischemia. *Cell* **118**, 687–698 (2004).
53. O. Yermolaieva, A. S. Leonard, M. K. Schnizler, F. M. Abboud, M. J. Welsh, Extracellular acidosis increases neuronal cell calcium by activating acid-sensing ion channel 1a. *Proc. Natl. Acad. Sci. U.S.A.* **101**, 6752–6757 (2004).
54. X. M. Zha, J. A. Wemmie, S. H. Green, M. J. Welsh, Acid-sensing ion channel 1a is a postsynaptic proton receptor that affects the density of dendritic spines. *Proc. Natl. Acad. Sci. U.S.A.* **103**, 16556–16561 (2006).
55. T. A. Green, M. T. Bardo, Opposite regulation of conditioned place preference and intravenous drug self-administration in rodent models: Motivational and non-motivational examples. *Neurosci. Biobehav. Rev.* **116**, 89–98 (2020).
56. M. A. Doyle, V. Bali, A. L. Eagle, A. R. Stark, B. Fallon, R. L. Neve, A. J. Robison, M. S. Mazei-Robison, Serum- and glucocorticoid-inducible kinase 1 activity in ventral tegmental area dopamine neurons regulates cocaine conditioned place preference but not cocaine self-administration. *Neuropsychopharmacology* **46**, 1574–1583 (2021).
57. J. A. Wemmie, J. Chen, C. C. Askwith, A. M. Hruska-Hageman, M. P. Price, B. C. Nolan, P. G. Yoder, E. Lamani, T. Hoshi, J. H. Freeman Jr., M. J. Welsh, The acid-activated ion channel ASIC contributes to synaptic plasticity, learning, and memory. *Neuron* **34**, 463–477 (2002).
58. T. Kristian, Isolation of mitochondria from the CNS. *Curr. Protoc. Neurosci.* **Chapter 7**, Unit 7.22 (2010).

59. J. A. Wemmie, C. C. Askwith, E. Lamani, M. D. Cassell, J. H. Freeman Jr., M. J. Welsh, Acid-sensing ion channel 1 is localized in brain regions with high synaptic density and contributes to fear conditioning. *J. Neurosci.* **23**, 5496–5502 (2003).
60. C. A. Schneider, W. S. Rasband, K. W. Eliceiri, NIH image to imageJ: 25 years of image analysis. *Nat. Methods* **9**, 671–675 (2012).

Acknowledgments: We thank A. Gutman and C. Cosme for the help and advice during the mouse cocaine-IVSA experiment. We thank C. Kreple for critical reading. We also thank G. Wang and M. Conlon for assistance. We thank the University of Iowa Central Microscopy Research Facility for using the Zeiss LSM710 confocal microscope for dendritic spine imaging; this instrument was funded from the NIH (SIG grant, S10RR025439). **Funding:** J.A.W. was supported by the National Institute of Drug Abuse (R01DA052953 and 5R01DA037216), Department of Veterans Affairs (Merit Award, IO1BX004440), and Roy J. Carver Charitable Trust. R.T.L. was supported by DA049139 and DA048055. **Author contributions:** Conceptualization: S.C.G., R.T.L., and J.A.W. Experiments, data collection, and analyses: S.C.G., A.G., R.J.T.-H., R.F., and J.B.H. Funding and administration: R.T.L. and J.A.W. Writing: S.C.G., A.G., R.J.T.-H., R.T.L., and J.A.W. **Competing interests:** The authors declare that they have no competing interests. **Data and materials availability:** All data needed to evaluate the conclusions in the paper are present in the paper and/or the Supplementary Materials.

Submitted 12 April 2022
Accepted 22 September 2022
Published 16 November 2022
10.1126/sciadv.abq5058